



HAL
open science

Etude des propriétés de transport du béton soumis à des chargements thermo-mécaniques différés

Matthieu Briffaut, El, Dandachy, Mohamad Ezzedine, Pont, Stefano Dal,
Frédéric Dufour

► To cite this version:

Matthieu Briffaut, El, Dandachy, Mohamad Ezzedine, Pont, Stefano Dal, Frédéric Dufour. Etude des propriétés de transport du béton soumis à des chargements thermo-mécaniques différés. CFM 2017 - 23ème Congrès Français de Mécanique, Aug 2017, Lille, France. hal-03465742

HAL Id: hal-03465742

<https://hal.science/hal-03465742>

Submitted on 3 Dec 2021

HAL is a multi-disciplinary open access archive for the deposit and dissemination of scientific research documents, whether they are published or not. The documents may come from teaching and research institutions in France or abroad, or from public or private research centers.

L'archive ouverte pluridisciplinaire **HAL**, est destinée au dépôt et à la diffusion de documents scientifiques de niveau recherche, publiés ou non, émanant des établissements d'enseignement et de recherche français ou étrangers, des laboratoires publics ou privés.

EFFECT OF CREEP IN TRACTION ON CONCRETE PERMEABILITY

M. Ezzedine El Dandachy, M. Briffaut, S. Dal Pont and F. Dufour

Univ. Grenoble Alpes, CNRS, Grenoble INP¹, 3SR, F-38000 Grenoble, France
E-mail: matthieu.briffaut@3sr-grenoble.fr

Abstract :

During a severe accident for reinforced concrete structures and especially nuclear power plant, coupled thermo-hygro-mechanical stresses may lead to the appearance of cracks. The overall leakage rate of a structure is governed by the combination of different permeabilities to concrete gases which are strongly in dependency with the mechanical and hydric state.

An experimental campaign is carried out to study the effect of differed strains (creep) on gas permeability of concrete. Traction (30 % the tensile strength) loadings at different temperatures (20, 100 and 180 °C) and ambient relative humidity are applied on dog-bone concrete samples. Loadings are maintained for two weeks to generate creep.

Permeabilities in longitudinal and radial directions with respect to load axis are addressed. The initial intrinsic permeability for companion cylindrical dried samples is found isotropic and equal to $2.93 \times 10^{-17} \text{ m}^2$. Results show that intrinsic permeability of samples under coupled effect of traction creep and temperature is found more significant in the radial direction. The normalized radial permeability could be higher than the normalized longitudinal one up to a ratio of 3.4.

Key words: Thermo-hygro-mechanical loadings, Creep, Gas permeability, Concrete.

1 Introduction

In case of a severe accident (SA), questions arise regarding the tightness of the concrete vessel mainly for the 1300 MW and N4 type of nuclear power plants where the confinement is fulfilled by the inner pre-stressed concrete vessel. The severe accident (SA) is defined by an inner pressure of 5 bars, a temperature of the vapour-gas mixing up to 180°C maintained during 2 weeks. The integrity of the structure is guaranteed since the pressure is lower than the design pressure. However, the tightness of the concrete vessel is affected by the micro-cracking induced by the coupled effects of different loadings due to the severe accident. In order to assess these questions, one has to better understand the hygro-thermo-mechanical behaviour and its consequences on the transfer properties of the pre-stressed concrete vessel accounting for material ageing (creep, relaxation, drying) and also during a SA.

Before the appearance of a localized crack, transport phenomena are governed by the porous network of the cementitious material and its degree of saturation. Drying shrinkage creates micro-cracks in concrete which alter the initial porous network and lead to permeability increase. This latter may induce permeability anisotropy in concrete structure depending on its geometry; for instance in walls longitudinal permeability is more significant than transversal one [1]. Furthermore, the temperature

¹ Institute of Engineering Univ. Grenoble Alpes

rise (above 140 °C) causes the departure of water that is chemically bounded to the hydrates of concrete [2, 3, 4], also amending its porous network (and its mechanical behavior) and could highly increase the gas permeability of concrete [5, 6]. In addition to the changes in the intrinsic properties of the cement paste, micro-cracks may be generated by the interaction between aggregates and cement paste as these two components have different thermal expansions and different stress-strain relationships [7]. Moreover, creep strains related to the increase in pressure and temperature within the containment during a severe accident will affect the material porous structure and will generate additional micro-cracks, thus increasing the leakage rate. Consequently, micro-cracks of different origins should be taken into account in the estimation of the intrinsic permeability of concrete. When a macro-crack appears due to micro-cracks coalescence, it becomes a preferential channel for the fluid and almost all of the leakage flows through this macro-crack [8, 9, 10, 11].

Studies in the literature have shown that the evolution of gas permeability of concrete is found to be exponential (or power law) with respect to temperature [12, 13]. The effect of temperature on gas permeability of ordinary concrete as well as the correlation on experimental tests was determined in [5]. However, the coupled effect of drying, temperature and mechanical loading on concrete permeability is still an open issue. Specially, when loadings could last for weeks as the case of a severe accident, creep strains will be developed.

In this contribution the effect of creep (in traction) at different temperatures on concrete permeability will be analyzed. Finally, the isotropic/anisotropic property of permeability will be studied for some of the specimens.

To this end, the experimental campaign consists of studying the effect of thermo-hygro-mechanical loadings and creep on the permeability in longitudinal and radial directions of VeRCoRs concrete (reference concrete for the national project MaCEnA) is conducted. Thermo-mechanical and creep tests are performed by collaborators in the project MaCEnA (“MAîtrise du Confinement d'une ENceinte en Accident”). The specimens are then conducted to permeability tests in 3SR laboratory. It should be pointed out, that the study of the permeability in this campaign is restricted to residual gas permeability measurements of dried specimens. All specimens are completely dried at 80 °C before the permeability tests.

2 Experimental program

2.1 Concrete formulation

The concrete studied in this contribution is the reference concrete for the national project MaCEnA (tightness assessment of confinement vessels during an accident). According to EDF (Electricité De France) and collaborators in MaCEnA, the compressive strength, the tensile strength and the Young's Modulus of VeRCoRs concrete are around 45 MPa, 3.85 MPa and 35 GPa at 28 days respectively. The different constituents and their quantities are given in Table 1.

Constituents	Quantity (kg/m ³)
Cement CEM I 52.5 N CE CP2 NF ‘GAURAIN’	320
Sand calcium silicates 0/4 Reconstuted mix LGP1 ‘GSM’ 0/4	830
Gravels calcium silicates 4/11 LGP1 ‘GSM’	445
Gravels calcium silicates 4/11 BALLOY ‘GSM’	550
Admixture SIKAPLAST TECHNO 80	2.4
Water	197.5

Table 1: Formulation of MaCEnA's concrete.

2.2 Specimens and loadings

The concrete specimens are all provided by the collaborators (EDF, CERIB and LMDC). After casting, all samples were conserved and cured following Rilem Tc 129 recommendations [14]. Figure 1 presents a diagram that summarizes the specimens that are dealt with in this experimental campaign (mechanical and thermos-mecanical loading are made by other laboratories). Many specimen geometries exist based on the loading type and the collaborator. Table 2 provides additional details regarding the number and geometry of the specimens as well as regarding the loading(s) application. In addition, Figure 2 shows some photos/graph of the specimens.

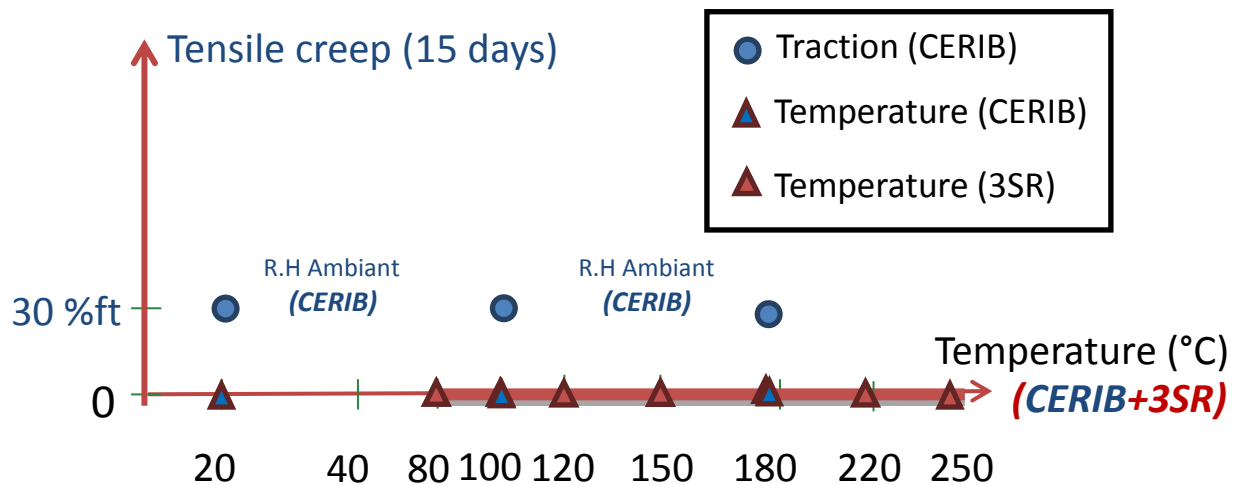
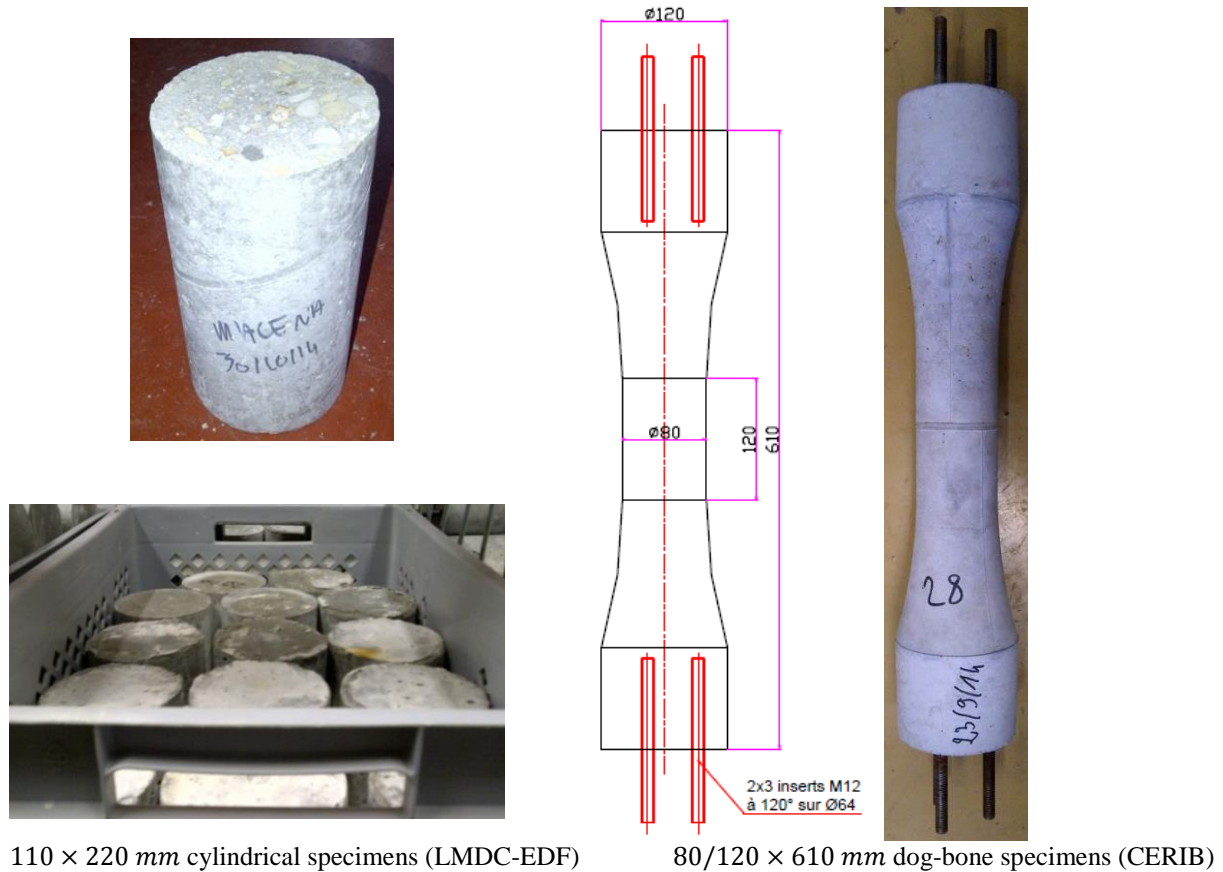


Figure 1: Diagram summarizes the specimens in project MACENA which undergo different hygro-thermo-mechanical loadings.

Specimen provider	Type of loading / (Physical phenomenon)	Specimens and slices	Application of loading(s)
LMDC-CERIB-EDF	No mechanical loading (drying shrinkage)	Cylindrical sound specimens (110 × 220 mm) (LMDC-EDF) cut each into slices of 50 mm length and 1 dog-bone sample (80/120 × 610 mm) is cut (in its effective part) into 3 slices of 40 mm length.	After slicing, slices are dried at 80 °C and ambient R.H. for initial permeability determination.
CERIB	Creep in traction (30 % f_t) for 14 days at 20°C (drying creep)	2 dog-bone samples (80/120 × 610 mm). Each dog-bone sample (in its effective part) is cut into 3 slices of 40 mm length.	The traction loading is applied to the dog-bone specimen (0.25 kN/s) at ambient R.H. Slicing is done after unloading. Slices are then dried at 80 °C for permeability tests.
CERIB	Creep in traction (30 % f_t) for 14 days at 100 and 180 °C (Load induced thermal strain)	2 dog-bone samples (80/120 × 610 mm) per temperature. Each dog-bone sample (in its effective part) is cut into 3 slices of 40 mm length.	The tensile loading is applied first to the dog-bone specimen (0.25 kN/s) at 20 °C. Heating to the desired temperature is then applied (1°C/min) at ambient R.H. Slicing is done after unloading. Slices are then dried at 80 °C for permeability tests.

Table 2: Summary of specimens and loadings that are dealt with in the experimental campaign.



110 × 220 mm cylindrical specimens (LMDC-EDF)

80/120 × 610 mm dog-bone specimens (CERIB)

Figure 2: Photos of the samples received from collaborators in project MACENA.

3 Permeability assessment

3.1 Permeability system

A general view of the permeability device is presented in Fig. 1. It is composed of:

- 1) Three mass flowmeters with different measuring range, the highest 25000 mln/min, the intermediate 750 mln/min and the lowest 20 mln/min. (n: normal conditions; 0°C, 1 atm)
- 2) Pressure regulator that controls accurately the gas pressure.
- 3) Gas reservoir of nitrogen (N₂) provided with a pressure reducer.
- 4) Permeability chamber (see Figure 4 for details). Note that the specimen holder is replaceable to fit with the specimen dimensions.
- 5) A PC for data acquisition.

This permeability device gives the possibility of testing concrete permeability in both longitudinal and radial directions thanks to the system shown in Figure 4. The configurations for the permeability test in longitudinal and radial direction are presented respectively in Figure 4b and Figure 4c. For practical purposes and due to technical limitations, the study is limited to residual permeability of completely dried specimens. Each permeability measurement is performed under controlled gas pressure of 1.5 to 3.5 bars.

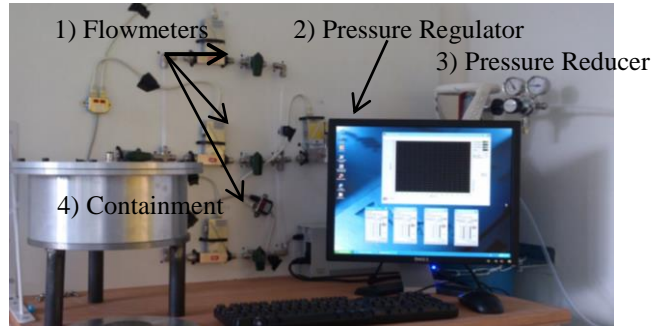


Figure 3: Permeameter device

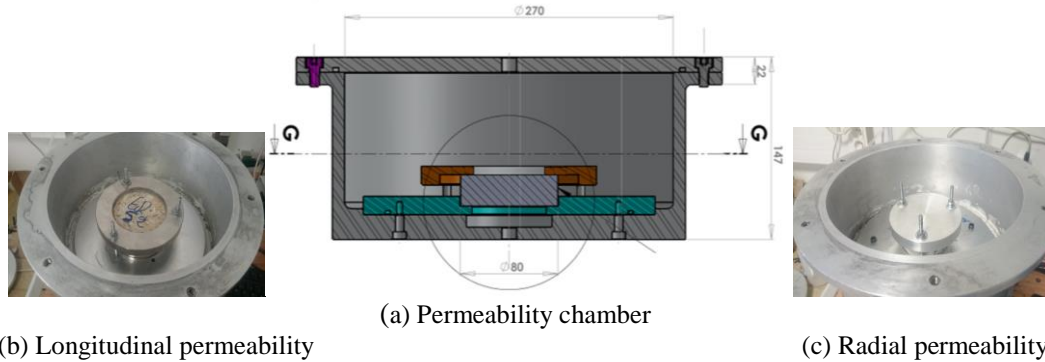


Figure 4: Technical draws of the permeability chamber (a), longitudinal permeability testing (b) and radial permeability testing (c).

3.2 Permeability calculation

The permeability test is performed by injecting gas in the permeability chamber under a given pressure. As shown on Figure 4, two ways for the gas injection are possible. Depending on the pressure gradient and the sealing of the specimen lateral surfaces, the gas injection is performed from the upper part or the bottom part of the permeability chamber. Due to practical reasons, the gas injection is carried out from bottom without the need to fill the whole permeability chamber. In this way, time to reach the permanent regime is lower (15 to 40 minutes depending on the gas pressure and specimen length).

Due to pressure gradient, gas percolates through concrete. Flux boundary conditions using aluminum foils are imposed on the samples to impose the percolation path, e.g. aluminum foil is placed on the lateral surface of the sample for the longitudinal configuration whilst it is placed on the flat surfaces for the radial configuration.

After verifying that the regime is laminar (linear evolution of the flow rate versus the gradient of pressure squared), the longitudinal apparent permeabilities k_{al} are calculated using Darcy's law [15] for compressible fluids (Nitrogen) (Equation (1)) and similarly for the radial apparent permeabilities k_{ar} (Equation (2)).

$$k_{al} = \frac{Q_i^l}{S} \frac{2\mu L P_{atm}}{(P_i^2 - P_{atm}^2)} \quad (1)$$

$$k_{ar} = \frac{Q_i^r}{\pi L} \frac{\mu \ln\left(\frac{r_2}{r_1}\right) P_{atm}}{(P_i^2 - P_{atm}^2)} \quad (2)$$

Where Q_i^l and Q_i^r are the inlet flow rates in the longitudinal and radial direction respectively. They are measured using the mass flowmeters and expressed in mln/min . It should be noted, that since the flowmeters are mass ones, the measured flowrates are already given under normal conditions and therefore P_{atm} (1.013 bar) must be used in Equations (1) and (2). Moreover, μ is the dynamic viscosity

of N_2 at 20°C, P_i is the gas pressure at the inlet, r_1 (m) is the radius of the hole for radial permeability test, r_2 (m) is the radius of the specimen, L (m) is the specimen length and S (m²) is the surface exposed to the flow.

It is well known that Darcy's law for compressible gases applied to concrete overestimates its intrinsic permeability, thus to find an intrinsic permeability of concrete Klinkenberg correction could be adopted [16]. It consists of performing permeability tests on concrete sample with different gas pressures leading to different apparent permeabilities. Then, by plotting the apparent permeabilities versus the inverse of the mean gas pressure, a linear fit is found if the flow is laminar. The linear regression of the fitted line until it intersects with the y-axis (for infinite gas pressure) gives the intrinsic permeability of the sample. For this campaign, at least four different pressures are used to apply Klinkenberg's method. A previous application of the Klinkenberg's method for the same concrete is shown in [17].

4 Effect of creep in traction on concrete intrinsic permeability

Previous results on initial reference permeability and effect of drying shrinkage and temperature on multi-directional concrete permeability were presented in [17]. Some of the results presented in [17] will be recalled for comparison. The effect of basic creep, drying creep and load induced thermal strain, in traction, on concrete permeability are presented in the following sections.

4.1 Effect of drying creep in traction on concrete intrinsic permeability

To study the effect of drying creep in traction on concrete gas permeability (with no thermal loading), two dog-bone samples (6 slices in total for permeability tests) are conducted for traction test at 30% of the tensile strength of the material and room temperature (20°C). The tensile loading is maintained for two weeks for possible drying creep generation. Permeability measurements show an average intrinsic permeability of 7.1×10^{-17} m² (6.0×10^{-17} m² to 8.2×10^{-17} m²) and 4.3×10^{-17} m² (3.0×10^{-17} m² to 6.3×10^{-17} m²) in both longitudinal and radial directions respectively. The values are found very similar to the initial permeabilities in both directions for slices from dog-bone samples (the anisotropy already seen for the unloaded dog-bone samples, it is caused by the drying due to structural hydric effect, see [17]). This shows that there is no significant effect of traction creep at 30% the tensile strength on the intrinsic permeability of concrete. Indeed, many authors have already shown for quasi-static load that at 30% of the tensile strength and below, the intrinsic permeability of the material is almost unaltered [18]. In addition, this study has shown that the drying creep in traction at 30% of the tensile strength and 20°C for 14 days did not affect the initial intrinsic permeability in both directions. Therefore, one can conclude that traction drying creep at 30% the tensile strength for 14 days did not induce a permeability increase at 20°C for VeRCorS concrete with respect to unloaded material.

4.2 Induced anisotropic permeability due to effect of load induced thermal strain in traction

The coupled effect of traction creep (30% of the tensile strength) and temperature (100 °C and 180 °C, mechanical load precedes the thermal one), applied for two weeks, on longitudinal/radial intrinsic permeability of concrete is presented in this section. This study is performed on four dog-bone samples (two samples per temperature). After the creep tests are done, samples are unloaded and then the effective parts of the samples were sliced into three slices (40 mm height, 80 mm diameter) each for permeability measurements (see section 2.2 for more details on specimens and loadings). It should be recalled that the initial intrinsic permeability of the material in this case is not isotropic due to effect of drying shrinkage (see [17]). Thus, to better compare the permeability evolutions in both directions, the normalized intrinsic permeability with respect to intrinsic permeability at 80 °C is considered. Unfortunately, for practical reasons within the MaCEnA project, the initial intrinsic permeabilities for the samples that had undergone creep and temperature of 100°C or 180°C were not assessed before the application of loadings. However, three other sound dog-bone samples were used to determine the initial intrinsic permeability in both directions (endogeneous curing conditions before

drying at 80°C). This procedure of normalization is certainly not perfect but allows to better compare the intrinsic permeability evolutions in both directions.

The evolution of the normalized intrinsic permeability in the longitudinal/radial direction versus temperature for concrete subjected to traction creep at 30 % of the tensile strength and ambient R.H for 14 days is presented in Figure 5. On this graph, mean value as well as maximum and minimal value are displayed. As discussed in section 4.1.1, the traction creep at 30% of the tensile strength and 20°C has no significant effect on intrinsic permeability of concrete. The ratios in both directions with respect to the initial permeabilities are very close to 1. However, when tensile loading is applied followed by temperature increasing above 100 °C, one can notice that the mean normalized radial permeability becomes significantly higher than the longitudinal one, especially at 180°C. It should be pointed out as well that for the same dog-bone sample (see Table 3) the permeabilities in the longitudinal direction are not much scattered. Whilst in the radial direction significant dispersion is noticed. This could be explained by the occurrence of one or more micro-cracks crossing a slice in the radial direction due to micro-cracks coalescence induced by the coupled effect of temperature and traction creep (load induced thermal strain). Micro-cracks are generated by temperature and then propagated more importantly in the radial direction due to traction creep. For those particular slices, the normalized radial permeability could be higher than the normalized longitudinal one up to factor of 3.4 (see Table 3). It must be highlighted, that the maximum radial permeability that corresponds to one slice of one of the dog-bone specimens that were subjected to the coupled effect of temperature (180 °C) and traction creep (30 % the tensile strength, 14 days) is equal to $39 \times 10^{-17} m^2$. Whereas, the maximum radial permeability recorded for the slices from dog-bone samples that undergone only temperature (180 °C) is equal to around $20 \times 10^{-17} m^2$ (see Figure 6) with mentioning that the traction creep (30 % the tensile strength, 14 days) alone did not affect the concrete permeability. This shows that there is additional micro-cracking caused by LITS that is developed which led to higher permeability in the radial direction.

Further work could be dedicated to use experimental technics in order to observe the cracking pattern in the slices such as X-ray or neutrons tomography for instance.

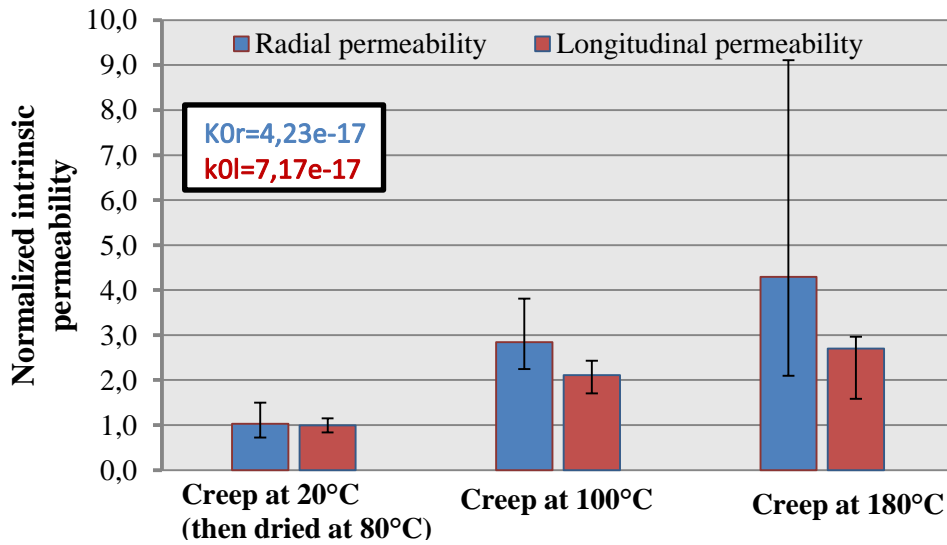


Figure 5: Evolution of the normalized intrinsic permeability under creep test versus temperature.

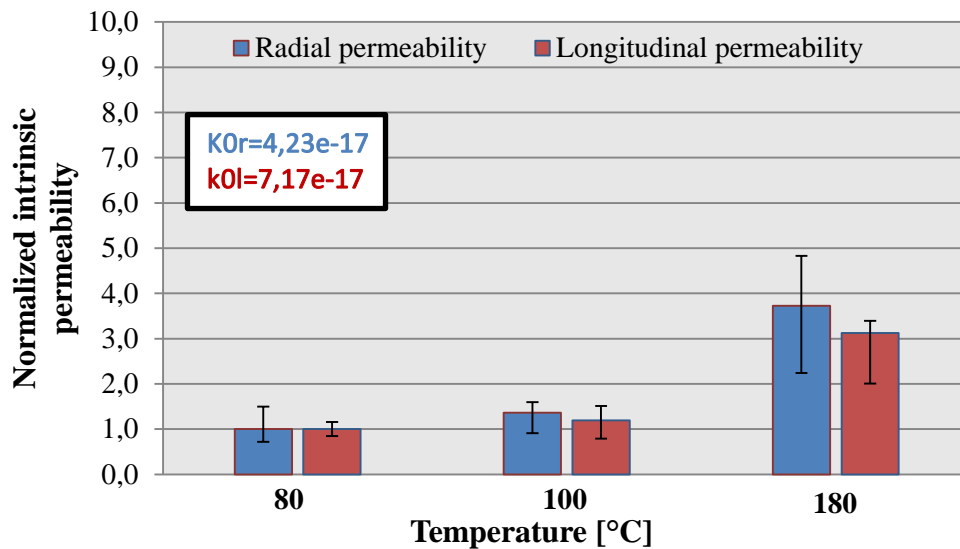


Figure 6: Evolution of the normalized intrinsic permeability versus temperature [17].

Slices (temperature 180°C)	Normalized longitudinal permeability nk_l	Normalized radial permeability nk_r	nk_r/nk_l
S1-center	2.96	2.17	0.73
S1-extremety1	2.7	9.11	3.37
S1-extremety2	2.43	5.49	2.26
S2-center	2.17	2.09	0.963
S2-extremety1	1.58	2.22	1.41
S2-extremety2	2.14	4.69	2.19

Table 3: Ratio of normalized radial to longitudinal permeability for concrete under creep in traction (30% tensile strength) at temperature of 180°C.

5 Conclusions

In this contribution, influence of creep in traction on intrinsic permeability of concrete in two directions, longitudinal and radial, are analyzed. Many conclusions could be drawn:

- Drying creep in traction at 30% the tensile strength, ambient temperature and relative humidity, for 14 days did not induce a permeability increase at 20°C for concrete with respect to unloaded material in both directions, longitudinal and radial.
- Intrinsic permeability of sample under coupled effect of traction loading (30% the tensile strength) and temperature (100 and 180 °C), applied for 14 days, is found more significant in the radial direction with respect to samples that only undergone thermal loading. This could be explained by a localization of micro-cracks crossing a slice in the radial direction caused by the presence of the tensile loading. Micro-cracks are generated by temperature and then propagated more importantly in the radial direction due to traction creep (load induced thermal strain). For those particular slices, the normalized radial permeability could be higher than the normalized longitudinal one up to a factor of 3.4. The intrinsic permeability in the radial direction in this case (for 30% the tensile strength and temperature of 180 °C) could reach a value of $39 \times 10^{-17} m^2$. Whereas the maximum radial permeability recorded for the slices from dog-bone samples that undergone only temperature (180 °C) is equal to around $20 \times 10^{-17} m^2$.

Further work could be dedicated to use experimental technics in order to observe the cracking pattern in the slices such as X-ray or neutrons tomography for instance.

Acknowledgements

The authors gratefully acknowledge the funding support from France's National Research Agency through "MACENA" project (ANR-11-RSNR-012). 3SR is part of the LabEx Tec 21 (Investissements d'Avenir – Grant agreement no. ANR-11-LABX-0030).

References

- [1] Nicolas Burlion, Frédéric Skoczylas, Thierry Dubois. Induced anisotropic permeability due to drying of concrete. *Cement and Concrete Research*, Elsevier (2003), 33 (5), pp.679-687.
- [2] Baroghel-Bouny V, Caractérisation des pâtes de ciment et des bétons; méthodes, analyse, interprétations, Edition du Laboratoire Central des Ponts et Chaussées, Paris, 1994.
- [3] Diederichs U., Jumppanen U.M., Penttala V, Behaviour of high strength concrete at high temperature, Espoo: Helsinki University of Technology, Report 92, 1989.
- [4] Noumowé A, Effet de hautes températures (20-600 °C) sur le béton. Cas particulier du béton à hautes performance, Thèse de Doctorat, INSA Lyon, 1995.
- [5] Choinska M, Khelidj A, Chatzigeorgiou G, Pijaudier-Cabot G. Effects and interactions of temperature and stress-level related damage on permeability of concrete. *Cem Concr Res* (2007); 37(1):79–88.
- [6] Zeiml, M., Lackner, R., Leithner, D. & Eberhardsteiner, J. Identification of residual gas-transport properties of concrete subjected to high temperatures. *Cement and Concrete Research* 38 (2008) 699–716.
- [7] Grondin F, Dumontet H, Ben Hamida A., Boussa H. Micromechanical contributions to the behaviour of cement-based materials: Two-scale modelling of cement paste and concrete in tension at high temperatures, *cement and concrete composites* (2010).
- [8] Picandet V, Khelidj A, Hervé B. Crack effects on gas and water permeability of concretes. *Cement and Concrete Research* 2009; 39(6): 537-47, DOI: 10.1016/j.cemconres.2009.03.009.

- [9] Akhavan A, Seyed-Mohammad-Hadi S, Farshad R. Quantifying the effects of crack width, tortuosity, and roughness on water permeability of cracked mortars. *Cement and Concrete Research* (2012); 42(2): 313-20, Doi:10.1016/j.cemconres.2011.10.002.
- [10] Rastiello G, Boulay C, Dal Pont S, Tailhan JL, Rossi P. Real-time water permeability evolution of a localized crack in concrete under loading. *Cement and Concrete Research* (2014); 56: 20-28, DOI: 10.1016/j.cemconres.2013.09.010.
- [11] Ezzedine El Dandachy M, Briffaut M, Dufour F, Dal Pont S. An original semi discrete approach to assess gas conductivity of concrete structures, *International Journal for Numerical and Analytical Methods in Geomechanics* 2016, DOI: 10.1002/nag.2655.
- [12] Bazant Z.P. et Thonghantai W., Pore pressure and drying of concrete at high temperature, *J. Eng. Mech. Div. (ASCE)* 104 (1978) 1059-1079.
- [13] Gawin D., Alonso C., Andrade C., Majorana C.E., Pesavento F., Effect of damage on permeability and hygro-thermel behaviour of HPCs at elevated temperatures: Part 1. Experimental results, *Computers and Concrete* (2005) 189-202.
- [14] RILEM TC 129-MHT, Test methods for mechanical properties of concrete at high temperatures, Part 1 Introduction, Part 2 Stress-strain relation, Part 3 Compressive strength, Part 4 Tensile strength, Part 5 Modulus of elasticity, Part 6 Thermal strain, Part 7 Transient creep, Part 8 Steady-state creep, Part 9 Shrinkage, Part 10 Restraint, Part 11 Relaxation.
- [15] Darcy H. Les Fontaines Publiques de la Ville de Dijon. Dalmont, Paris. 647 p. & atlas, 1856.
- [16] Klinkenberg L.J., The permeability of porous media to liquid and gaz, American Petroleum Institute, Drilling and Production Practice, pp. 200-213, 1941.
- [17] Ezzedine El Dandachy M, Briffaut M, Dal Pont S, Dufour F. Induced anisotropic gas permeability of concrete due to coupled effect of drying and temperature, *Key Engineering Materials*, 711: 871-878, 2016, DOI: 10.4028/www.scientific.net/KEM.711.871.
- [18] Hoseini M, Vivek B, Nemkumar B. The Effect of Mechanical Stress on Permeability of Concrete: A Review. *Cement & Concrete Composites* (2009); 31(4):213-20. doi:10.1016/j.cemconcomp.2009.02.003.